

1 Design and fabrication of neuroelectronic device containing gold 2 pyramid electrodes

3 Gymama Slaughter*^{a,b}, Joel Tyson^a, , Matthew Robinson^c, Chen J. Zhang^c, Minhquan
4 Tran^a

5 ^aBioelectronics Laboratory, University of Maryland Baltimore County; ^bDepartment of Computer Science and
6 Electrical Engineering, 1000 Hilltop Circle, Baltimore, MD, USA 21250;

7 ^cCenter for Nanoscale Science and Technology, National Institute of Standards and Technology Gaithersburg, MD,
8 USA, 20899
9

10 **Abstract.** A neuroelectronic device containing an electrochemically deposited multi-walled carbon nanotube
11 (MWCNT) sensitive layer was designed, fabricated and characterized. The neuroelectronic device consists of a
12 flexible polyimide substrate bearing four shanks with 16 gold rectangular pyramid electrodes per shank and
13 MWCNT sensitive layer. Each of the 16 gold pyramid electrodes with a top active area of 6 μm x 60 μm and depth
14 of 750 μm are positioned with a vertical separation distance of 100 μm on a shank width of 40 μm . Gold rectangular
15 pyramid electrodes are selected as the recording electrodes to enhance the electroactive surface area.
16 Electrochemical impedance spectroscopy (EIS) analysis of the resulting 16 gold pyramid electrodes on one of the
17 shanks of the neuroelectronic device was characterized at the physiological relevant frequency of 1 kHz. The
18 experimental results show that the gold electrodes are uniformly coated with MWCNTs sensitive layer. With no
19 MWCNT coating, the impedance response at 1 kHz could reach as high as 17.16 M Ω on average. Additionally, the
20 MWCNT coated gold pyramid electrodes exhibited a significant reduction in electrode impedance at 1 kHz to 45.73
21 k Ω on average demonstrating MWCNT ability to lower the impedance of the electrodes by roughening the electrode
22 surface.

23
24 **Keywords:** Microfabrication, polyimide, flexibility, neural probes, electrochemical impedance spectroscopy.

25
26 *Corresponding Author, E-mail: gslaught@umbc.edu
27

28 1 Introduction

29 Neuroelectronic devices used for the integration of neurons with electrodes in neurological
30 studies have enabled a better understanding of the complex neurological processes in animals
31 and in humans. Electroencephalography (EEG), electrocorticography (ECoG), local field
32 potential (LFP) and single-unit recordings are the four main technologies employed to stimulate
33 and record electrical signal from targeted neural tissues, and are particularly useful for
34 elucidating the complex processes that contributes to the onset of neurodegenerative diseases^{1,2}.
35 However, these technologies suffer from a number of limitations such as relatively low
36 resolution and are not suitable for use in recording brain activity from multiple sites deep within

37 the brain. The application of micro- and/ or nano-electromechanical systems (MEMs) or (NEMs)
38 to the fabrication of LFPs or single-units recording electrodes have led to the development of
39 minimally-invasive high density neuroelectronic devices that are designed to penetrate the pia
40 and maintain intimate contact with neurons. Electrode characteristics such as size, electrical
41 impedance, and the electrode's ability to achieve intimate contact with a neuron play a key role
42 in differentiating LFPs from single-units recordings³.

43 The current metal stereotrodes, tetrodes and microwire arrays employed are only capable
44 of recording activity at their exposed distal tips and the number of recording electrodes that can
45 be incorporated in these devices are limited⁴. A key challenge that remains to be addressed is the
46 reduction in the probe size while maintaining a large density of recording electrodes in order to
47 minimize tissue damage, scarring and device encapsulation. An advantage of using silicon based
48 microelectronics and/ or MEMs based fabrication techniques is that it can effectively reduce the
49 probe size and address the limitations of conventional metal microwire based neuroelectronic
50 devices⁵ in addition to the fact that it can be batch processed and yield reproducible planar or
51 three-dimensional electrode geometries⁶. However, these silicon-based electrodes are also prone
52 to host immune responses^{7,8} that eventually cause the recording signal to degrade during the
53 operation of the electrodes. Neuroelectronic devices based on polymers have been recently
54 demonstrated to offer an alternative to silicon based devices due to their mechanical (flexibility)
55 and chemical (biocompatible)⁹ properties. These devices can easily conform to the surrounding
56 brain tissue¹⁰, thus minimizing inflammation due to micromotion and tissue damage and improve
57 the device overall biocompatibility^{11,12}.

58 In order to acquire high quality signal when implanted, it is important that the impedance
59 of the recording electrode is optimal for the recording and stimulation of brain cells or tissues.

60 Neuroelectronic devices that exhibit high electrode impedance increases the electrode noise
61 profile, which further obscures recorded neuronal signals¹³. Therefore, it is important to employ
62 neuroelectronic devices with electrode sites that have low electrical impedances and high signal-
63 to-noise ratio to enable the acquisition of high quality recording signals from targeted neural
64 cells or tissues. Xiang et al demonstrated the reduction of gold electrode impedance
65 characteristics via the electrochemical deposition of multi-walled carbon nanotubes
66 (MWCNTs)¹⁴. The deposited MWCNTs provided a roughened sensitive layer that have been
67 shown to detect dopamine via cyclic voltametry^{14,15} and improve the quality of neuronal cell to
68 electrode adhesion¹⁶.

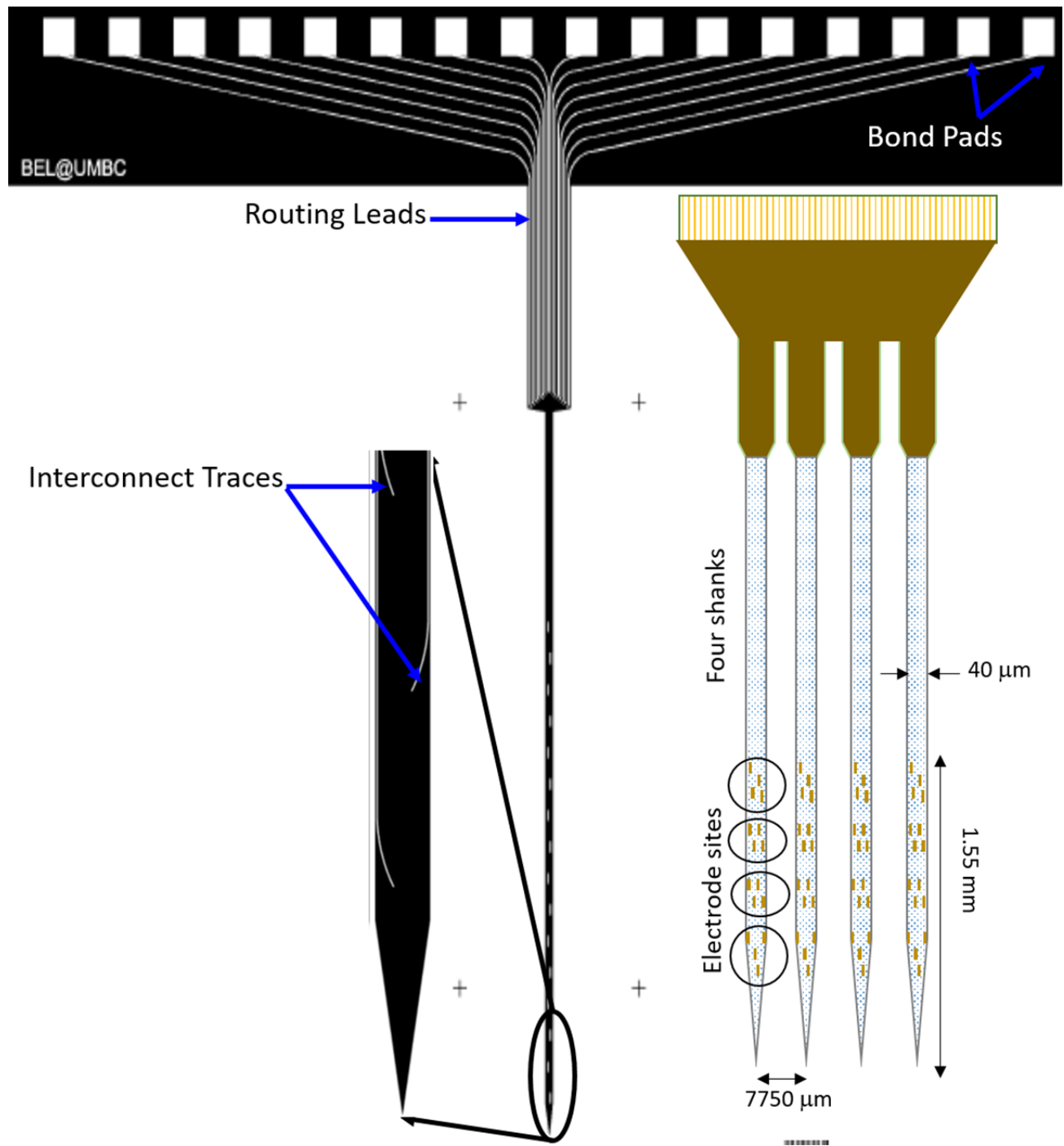
69 In this paper, we took advantage of the flexibility and biocompatibility of polymers to
70 design and fabricate polyimide based neuroelectronic device. Thin MWCNT coated gold
71 pyramid electrodes were employed to reduce the electrode impedance. The detailed design,
72 development and fabrication of such fully integrated neuroelectronic device is described and
73 discussed.

74 **2 Experimental Results and Discussion**

75 *2.1 Flexible Neuroelectronic Probe Design*

76 The flexible polyimide neurotronic probes are designed to use silicon substrate to provide initial
77 mechanical support, from which the flexible probe substrate is released and integrated with
78 interconnect cable. The 64-site flexible multi-shank neuroelectronic probes are constructed by
79 sandwiching the electrical interconnect traces in between two polyimide layers. These
80 interconnect traces connect the small electrodes sites to the large bond pads and is made from
81 chromium (Cr) thin film and gold (Au) thin film. The two polyimide layers consist of 1) an

82 insulating layer of HD-4104 (HD Microsystems, USA) polyimide (PI1) to structurally connect
83 the electrodes sites and bond pads, but electrically isolate them and 2) a final passivation layer of
84 HD-8820 polyimide (PI2) to serve as the final structural material and passivation for the
85 interconnect traces. Figure 1 presents the probe architectural design where four shanks are
86 protruding from the wider base platform. The multi-shank probe is made up of two metallization
87 layers: the first metallization layer forms the exposed 64 electrode sites and bond pads and the
88 second metallization carries the insulated interconnect traces. The metallization layers are
89 separated by a thin PI1 film. This architecture enables the packing of 16 electrodes per shank.
90 The shank width is 40 μm , widening to 250 μm at the base platform. The probe thickness is
91 approximately 8 μm . The shank length is 3 mm and the shanks are spaced at 7750 μm with 16
92 electrode sites on each of shanks. The electrode sites have top area of 6 μm x 60 μm and
93 thickness of 750 μm and distributed with 100 μm pitch. Additionally, the key design elements of
94 the probe structure are: the fine tip pyramidal shaped electrodes, 30° tapered polyimide shanks
95 for penetration into neural tissue, and the narrowly spaced gold interconnect traces.



96

97

98

Figure 1. Schematic design of the flexible neuroelectronic probe structure and CAD layout showing the electrode sites, interconnect traces and bond pads.

99 2.2 *High-Density Electrode and Probe Fabrication*

100 A flexible gold rectangular pyramid neuroelectronic probe platform is fabricated using flexible
101 biocompatible polyimide¹⁷. Figure 2 illustrates the fabrication sequence employed to translate the
102 gold pyramid electrodes into a flexible multi-shank neural probe in a cross-sectional view. Five
103 photolithographic masks are used to fabricate the probes on a 4-inch silicon wafer. The p-type
104 (100) silicon wafer is purchased from WRS Materials. The electrodes contain two metallization
105 layers. The first metallization forms the gold pyramid recording electrodes and bond pads and
106 the second metallization defines the interconnection traces. Polyimide (HD-4104) is used as the
107 insulation layer for the electric interconnection traces on the front side and are necessary to block
108 ionic current flow due to HD-4104 high electrical resistivity ($\sim 10^{16} \Omega\text{cm}$)^{18,19}. Both negative
109 (HD-4104) and positive (HD-8820) polyimide are used as the dielectric and structural material
110 respectively for the probe manufacturing because together they provide better mechanical
111 stiffness and flexibility for probing neurons.



1) Oxide deposition and patterning



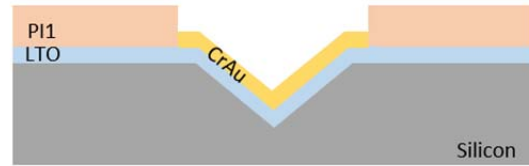
2) Silicon KOH etching to form V-groove



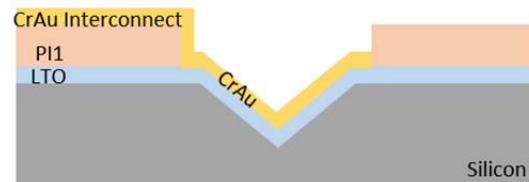
3) Silicon Oxide stripping and LTO deposition



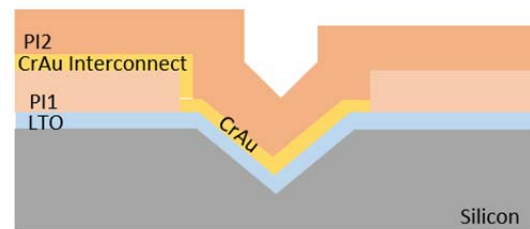
4) PI1(HD-4104) coating and patterning



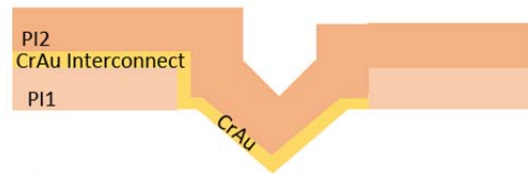
5) CrAu electrodes patterning and deposition



6) CrAu interconnect patterning and deposition



7) PI2(HD-8820) coating and patterning



8) LTO etching and final device releasing from silicon

112

113 Figure 2. Schematic illustration of the major processing steps in the fabrication of the 64-site probe.

114

115 A 200 nm thermal oxide is grown on the silicon wafer to serve as a mask for anisotropic etching

116 of silicon using potassium hydroxide (KOH). Photoresist patterning (standard S-1813 recipe

117 using MA6/MA8 mask aligner) is employed to create a mask for etching the SiO₂ with buffer

118 oxide etchant. The silicon is then etched with KOH to form the inverted rectangular pyramid

119 cavity to enable the molding of the gold rectangular electrode sites inside the inverted pyramid

120 cavity. Upon stripping the SiO₂ layer, a blanket 600 nm LTO is deposited and serves as the

121 sacrificial layer for final release of the probe. HD-4104 is photolithographically patterned on the
122 silicon substrate to expose the inverted pyramid cavity and to define the bond pads as well as
123 serve as the insulation layer for the second metallization layer. After curing the polyimide, the
124 polyimide film measures approximately 2-4 μm thick depending of the curing processing details.
125 NR9-6000PY is photolithographically patterned on top of the polyimide to expose the electrodes
126 and associated bond pads. The first metallization layer composed of 20 nm chromium and 750
127 nm is then deposited. The chromium layer is designed to provide adhesion between gold and
128 LTO. The gold electrodes and associated bond pads are e-beam evaporated to a thickness of 750
129 nm from a 99.99% pure gold target. Gold (Au) is selected as the electrode material due to its
130 chemical inertness, and compatibility with brain tissue^{20,21}. The second metallization layer of
131 Cr/Au (20 nm/ 250 nm) is e-beam evaporated and designed for the interconnection traces. The
132 interconnect traces are photoresist patterned and etched via ion milling to connect the electrode
133 sites to the bond pads. After interconnect traces fully patterned, a second polyimide layer HD-
134 8820 is spin coated, patterned to define the outer geometry of the devices and insulate the
135 interconnect traces as well as serve as the structural material. This is then followed by the
136 complete etching of the 600 nm LTO layer in buffer oxide etchant for the final release of the
137 flexible neuroelectronic probe. The chrome surfaces on the electrode sites and bond pads are
138 then removed by carefully dipping the probe in a chromium etchant solution while monitoring
139 the etch process under a microscope. The chromium etched probes are cleaned with Isopropanol
140 and DI water.

141 *2.3 Process development and integration challenges*

142 The polyimide based neuroelectronic probe fabrication was carried out on a 4-inch silicon
143 substrates. Polyimide serves as structural, insulating, and passivating layers for the device. Both

144 negative and positive polyimides selected provide mechanical flexibility, chemical stability, and
145 biocompatibility. In addition, they both exhibit the lowest moisture uptake of 0.5% and are
146 expected to provide excellent biostability by minimizing possible failure due to moisture
147 absorption. As for the metallization layers, gold was chosen for its biocompatibility and process
148 compatibility. The characteristic pyramid profile of the electrode was achieved via anisotropic
149 etching of $5\ \mu\text{m} \times 50\ \mu\text{m}$ features patterned on the silicon wafer with KOH. The bias introduced
150 by KOH in these features and the alignment marks resulted in several process challenges
151 downstream, wherein subsequent features were not perfectly aligned. To resolve this challenge,
152 it was important that the mask used (Step 1; Figure 2) was aligned flush with the wafer during
153 UV exposure to ensure minimum KOH bias. Additionally, the first polyimide layer PI1 (Step 4;
154 Figure 2) was designed to create a larger $6\ \mu\text{m} \times 60\ \mu\text{m}$ openings to account for this bias in the
155 electrode features and any undercutting that may occur during the wet-chemical etch process.
156 The $10\ \mu\text{m}$ routing leads, bond pads and electrode sites were formed on a single metallization
157 layer (Step 5; Figure 2). However, the wet etching of Cr/Au resulted in an interface-activated
158 undercutting of the resist film and openings between some of the routing leads and the bond
159 pads. Although the use of $10\ \mu\text{m}$ routing leads with a wider opening toward the bond pads were
160 found to eliminate the openings observed between these features, the electrode site features were
161 still defective. To circumvent this problem, we employed e-beam lift-off process using negative
162 resist to eliminate the undercut problem.

163 Moreover, the thick polyimide/metal stack posed challenge for process integration. In
164 order to ensure continuous electrical flow between the pyramid gold electrode and bond pad,
165 blanket Cr/Au deposition follow by ion milling was developed over the thick polyimide to form
166 the interconnect traces (Step 6; Figure 2). The interconnect traces were designed to overlap the

167 10 μm routing leads and the electrode sites. During the initial ion milling process development,
168 complete etching of the Cr/Au was not achieved, thereby impacting the functionality of the final
169 device. A descum step using reactive ion etching (RIE) was adopted to remove any residual
170 photoresist thus enable the Cr/Au to be fully etched. As a result, the ion milling process produced
171 interconnect traces with a width and spacing as narrow as 1 μm on certain portions of the shank.
172 Final device was formed by releasing shanks from the silicon substrate using buffer oxide
173 etching. The final shank formed has thickness of 8 μm and width of 40 μm . These shanks are
174 tapered at angle of 30° and exhibit flexible properties. Thereby, flexible gold pyramid electrode
175 probes with a Young's Modulus of 8.5 GPa are realized. The flexibility afforded by the probe
176 enables the shanks to bend when in contact with neural tissue, thus minimizing neural tissue
177 damage.

178 Scanning electron microscopy (SEM) micrographs of the 16-site electrodes per shank are
179 shown in Figure 3. A shank width of approximately 40 μm accommodates 16 channels. The
180 thickness of the shank varied from 6-10 μm . The shank length of 3 mm is necessary to allow
181 access to specific target of neural clusters within the brain tissue. The probe tip has a sharp angle
182 of 30° to enable easy penetration where the insertion force is concentrated at the end of the
183 probe. The shanks are placed 7750 μm apart and all the electrode sites are positioned within a
184 1.55 mm vertical coverage in order to increase the probability of recording neural signals from
185 multi-target neural clusters. The insert of Figure 3 depicts a close up view of the tip of the shank
186 and subsequently the electrode site, rectangular pyramid structure. This pyramidal structure
187 increases the conductive surface available for signal acquisition similar to that observed for
188 nano-composite surfaces [13].

189
190
191
192
193
194
195
196
197
198
199
200
201
202
203
204
205
206
207
208
209
210
211
212
213
214

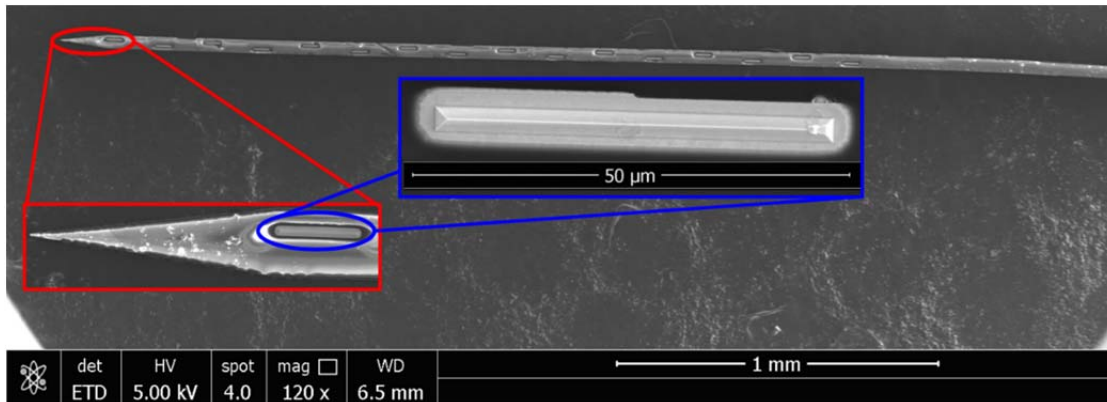
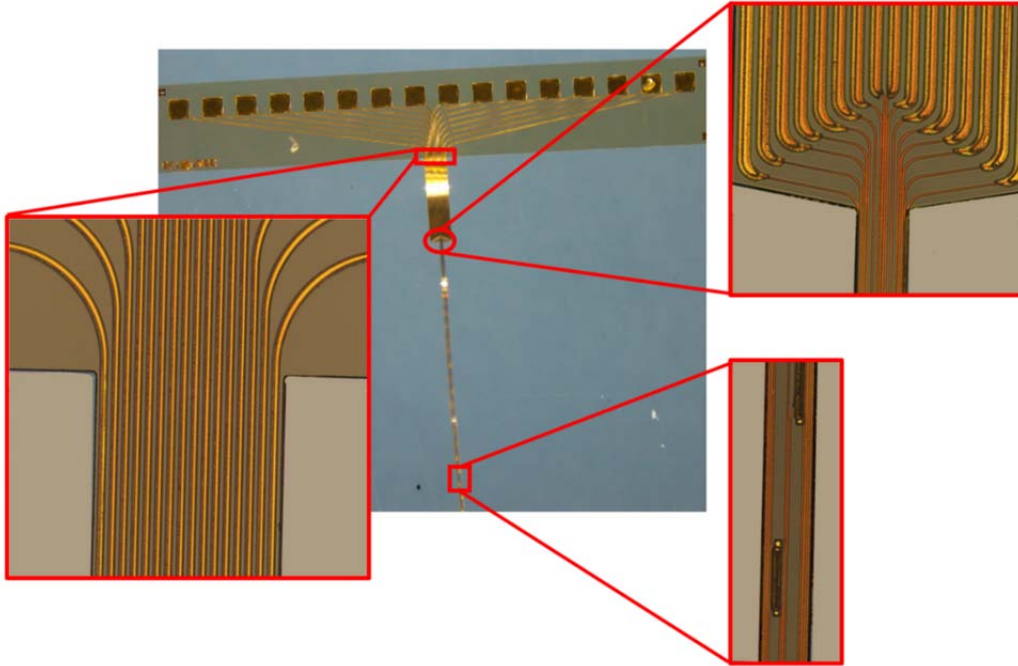


Figure 3. SEM micrographs of neuroelectronic probe shank with 16 recording electrode sites and submicron interconnect traces sandwiched between two polyimide layers and insert views of shank tip and rectangular pyramid shaped electrode.

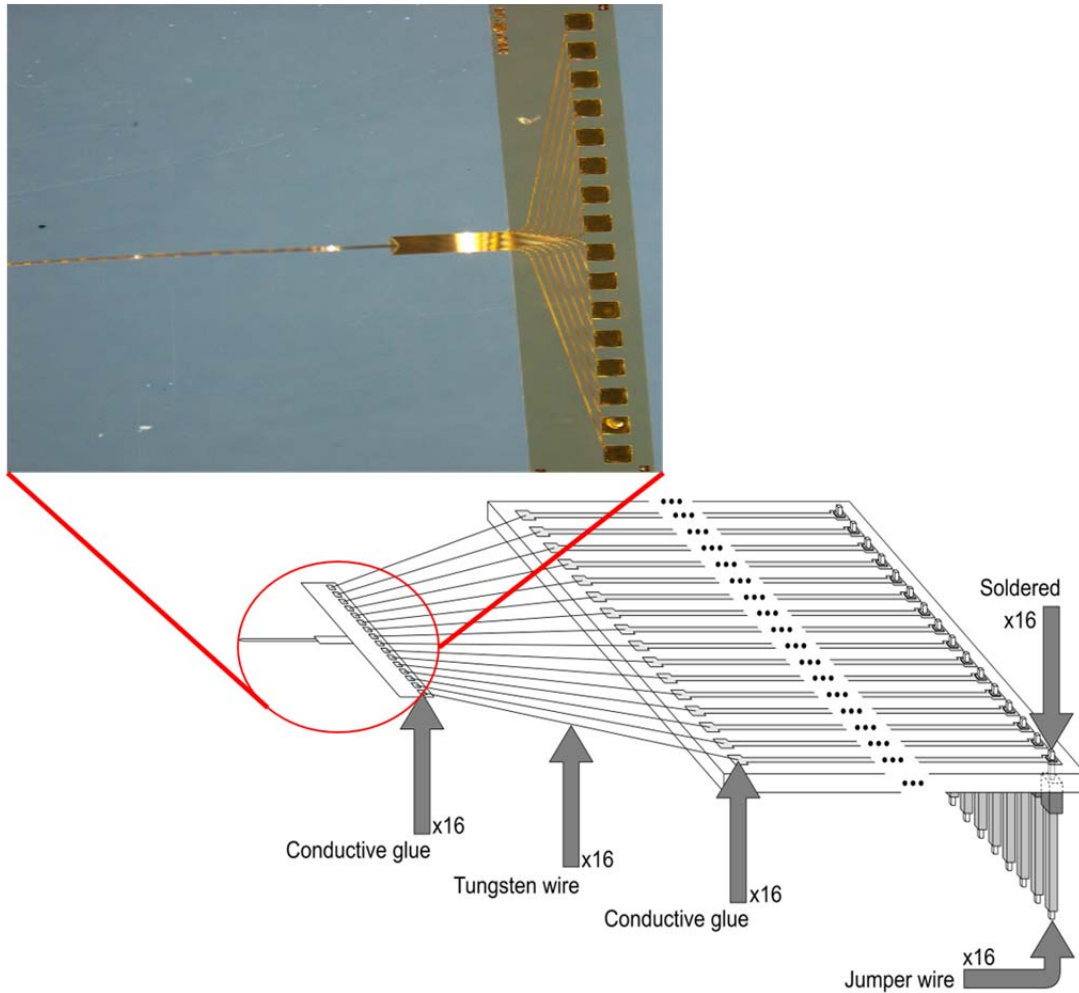
The probes that are acceptable for testing are identified by visual inspection under a microscope, and by electrochemical impedance spectroscopy (EIS) to assure electrical isolation of the electrode sites. Optical images of the fabricated probes are shown in Figure 4. To isolate the interconnect traces of the device from the aqueous environment, the traces were sandwiched between two biocompatible polyimide layers with low liquid permeability. The polyimide layers show very good adhesion. No visible delamination or defect due to adhesion is found between the first polyimide (HD-4104) layer and the second polyimide (HD-8820) layer, nor between the two polyimide layers and the gold electrode sites, interconnect traces and bond pads. The present yield indicates that about 90% of the fabricated probes pass these initial tests and can be suitable for impedance characterization and neural recording. As shown in Figure 4, the surface of the gold interconnect traces and electrode sites are smooth and reflective, whereas the polyimide surface appears dark due to light absorption by the polymer resin.



215
216 Figure 4. Flexible and optically transparent polyimide neuroelectronic probe accommodates associated bond pads,
217 interconnect traces 10 μm to 1 μm in two distinct metallization layers, and the traces are connected to the electrode
218 sites.

219 *2.4 Device Packaging*

220 The optical image in Figure 5 displays a clear view of the fabricated interconnects, bonding pads
221 and electrode sites on a single shank equipped with 16 gold recording electrode sites. For ease of
222 interfacing the flexible polyimide neuroelectronic probe to the measurement equipment, a printed
223 circuit board (PCB) consisting of interconnect lines is fabricated and connected to the probe
224 contact pads via tungsten wires ($\phi \approx 200 \mu\text{m}$). The tungsten wires were manually affixed with
225 conductive silver wire glue to the bonding pads in order to create a secure electrical connection.
226 Finally, a group of jumper wires were soldered to the distal end of the PCB for further wire
227 extension.



228

229 **Figure 5:** Flexible and optically transparent polyimide neural probe packaging.

230 *2.6 Electrochemical Impedance Spectroscopy*

231 The shank of probe was mounted in a test fixture and the probe was then immersed beyond
 232 the uppermost electrode site in a phosphate buffer saline (PBS) to mimic the physiologic
 233 environment at 37 °C and pH 7.4. The EIS experiment was performed with a potentiostat
 234 PGSTAT204, Metrohm Autolab to determine the electrode site impedance before and after
 235 MWCNT deposition. A three-electrode cell configuration with a Ag/AgCl electrode as the
 236 reference electrode and platinum electrode as the counter electrode was used. The probe was left
 237 in solution for 45 minutes before acquiring each impedance recording in triplicates. The

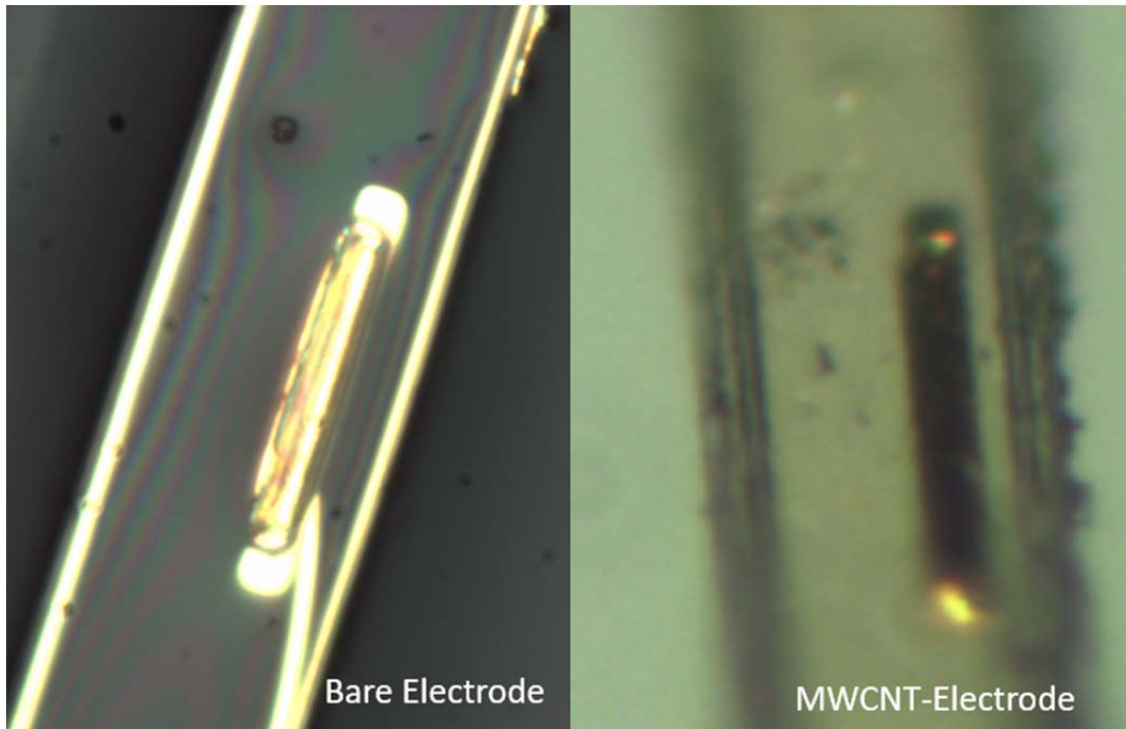
238 electrochemical impedance measurements were taken with a frequency range between 0.1 Hz –
239 10 kHz using a 10 mV peak-to-peak waveforms in order to identify stabilized probe site
240 impedances. The electrode impedance was observed to be on average approximately 135 k Ω (n =
241 24) at 1 kHz. In addition, the impedance was observed to gradually increases with decreasing
242 frequency. The impedance values obtained for the gold electrode sites are attributed to the
243 pyramidal geometry of the recording site electrode. The impedance value is well below most
244 values reported for non-surface treated neural probes²². Moreover, observed failed sites
245 (impedance out of range) are usually due to open interconnect traces or over etched traces. Post
246 failure SEM micrograph of probes appear to indicate open interconnect traces caused by
247 fabrication as the major cause for the failed sites.

248 *2.5 Multi-walled carbon nanotube (MWCNT) deposition*

249 The gold recording pyramid electrode surfaces were roughened with MWCNT in order to
250 increase the electrocatalytic surface area for cell adhesion and sensing, in addition to lowering
251 the overall electrode impedance. MWCNTs concentration of 1mg/mL was prepared using gold
252 sulfite electrolyte solution. The prepared solution was sonicated for 1 hour prior to
253 electrochemical deposition. The probe shank was assembled in a test fixture and to isolate the
254 gold bond pads of the device from the liquid test fixture environment, the tungsten wires and the
255 upper section of the probe were encapsulated with a biocompatible epoxy low water
256 permeability. MWCNT were deposited on six electrodes subsequently using each of the
257 recording electrodes as the cathode. A platinum wire electrode was used as the anode. The anode
258 and cathode were then connected to a function generator (Agilent 33250A). A monophasic
259 voltage pulse of 1.2 V, 10 Hz, at 50% duty cycle was applied for 1 minute. After the deposition
260 cycles, multiple layers of MWCNTs with gold nanoparticles were deposited on each of the gold

261 recording electrode sites on the shank. The optical images of the flexible polyimide probe shank
262 tip pre and post-MWCNT deposition are shown in Figure 6. The surface of the rectangular gold
263 electrode appears smooth and reflective, whereas the MWCNTs coated electrode surface
264 appeared rough and dark.

265



266 **Figure 6:** Recording electrode site before (left) and after (right) MWCNT deposition.

267

268 Figure 7 shows the comparison of the electrode impedance before and after MWCNT deposition.

269 The relatively large impedance value of 17.16 M Ω at 1 kHz on average is attributed to the

270 electrode area being covered by a small amount of the biocompatible epoxy used to affix the

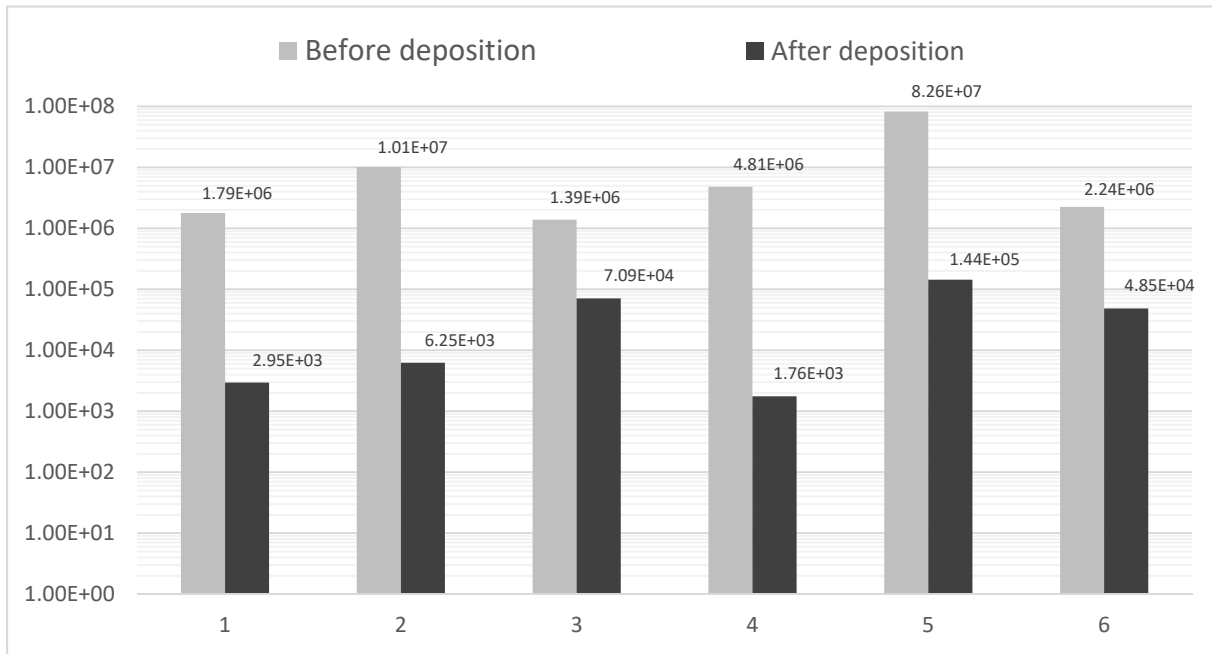
271 flexible probe shank to the borosilicate glass during the construction of the test fixture chamber.

272 The 60 seconds long deposition of MWCNTs resulted in a significant decrease in the overall

273 impedance. The average impedance at 1 kHz after MWCNT deposition was 45.73 k Ω . Clearly,

274 the MWCNTs contribute to the decrease of the electrodes electrical impedance. Thereby

275 resulting in an enhancement of charge storage capability²³. The observed average impedance
 276 after MWCNT deposition is an acceptable impedance value for electrochemical sensing of
 277 dopamine¹⁴.
 278



279 **Figure 7.** EIS measurement of six electrodes on a single probe shank before and after MWCNT deposition on a
 280 logarithmic scale.

281 This work is the first to demonstrate the use of standard microfabrication processes to fabricate
 282 multi-site neural probes with polyimide as supporting/structural and insulating/protective layers.
 283 Polyimide is an excellent alternative because it exhibits high electrical resistivity, mechanical
 284 flexibility, and biocompatibility properties. In addition, polyimide is known to not hydrate over
 285 time, which will eventually improve the probes' usefulness for chronic neural recording. The
 286 flexible neuroelectronic probe as described herein contains two polyimide layers as the insulating
 287 and structural material. The probe is approximately 8 μm thick and contains 64 pyramidal shaped
 288 electrode sites. The device was successfully integrated and the process development challenges
 289 were overcome by employing lift-off process to eliminate metal undercut, ion milling process to

290 create good step coverage of Cr/Au layer over the thick polyimide, and RIE descum process to
291 remove resist residual and resolve thin interconnect traces. The polyimide probe structure is
292 fabricated using standard microfabrication technology and does not require advanced CMOS
293 processing techniques. The flexibility afforded by the probe should increase the ruggedness of
294 the probe in various chronic neural recording applications. Additionally, we successfully
295 demonstrated the reduction of the gold recording electrodes' impedance via the electrochemical
296 deposition of MWCNTs. The observed impedance values at physiologically relevant frequency 1
297 kHz were on average 45.73 k Ω), which is suitable for electrochemical sensing.

298 *Disclosures*

299 The authors have no conflicts of interest.

300

301 *Acknowledgments*

302 The authors acknowledge the financial support of the National Science Foundation, United
303 States (Award ECCS-# 1342912). The infrastructure used for this work would not have been
304 possible without the significant contributions of the Center for Nanoscale Science and
305 Technology, National Institute of Standards and Technology Gaithersburg, MD, USA, and the
306 FEI SEM of the NanoImaging Center at the University of Maryland Baltimore County.

307 *References*

- 308 1. G.E. Slaughter, E. Bieberich, G.E. Wnek, K.J. Wynne, and A. Guiseppi-Elie, "Improving neuron-to-
309 electrode surface attachment via alkanethiol self-assembly: an alternating current impedance study,"
310 *Langmuir*, **20**(17), 7189-7200 (2004).

- 311 2. M. HajjHassan, V. Chodavarapu, and S. Musallam, “NeuroMEMS: neural probe microtechnologies,”
312 *Sensors*, **8**(10), 6704-6726 (2008).
- 313 3. M.Y. Chenget al., “A low-profile three-dimensional neural probe array using a silicon lead transfer
314 structure,” *Journal of Micromechanics and Microengineering*. **23**(9),095013 (2013).
- 315 4. S. Herwik et al., “Fabrication technology for silicon-based microprobe arrays used in acute and sub-
316 chronic neural recording,” *Journal of Micromechanics and Microengineering*. **19**(7), 074008 (2009).
- 317 5. J.F. Hetke and D.J. Anderson, D.J., “Silicon microelectrodes for extracellular recording” in Handbook
318 of neuroprosthetic methods, W.E. Finn and P.G. LoPresti, Eds., CRC Press, Boca Raton, chapter 7
319 **2003**.
- 320 6. A.K. Koivuniemi, S.J. Wilks, A.J. Woolley, and K.J. Otto, “Multimodal, longitudinal assessment of
321 intracortical microstimulation,” *Progr. Brain Res.* **194**, 131–144 (2011).
- 322 7. M.P. Ward, P. Rajdev, C. Ellison, and P.P. Irazoqui, “Toward a comparison of microelectrodes for
323 acute and chronic recordings,” *Brain research*. **1282**, 183-200 (2009).
- 324 8. J. Subbaroyan, D.C. Martin, and D.R. Kipke, “A finite-element model of the mechanical effects of
325 implantable microelectrodes in the cerebral cortex,” *Journal of neural engineering*, **2**(4), 103 (2005).
- 326 9. J. Tyson, M. Tran, and G. Slaughter, “Biocompatibility of a Novel Quad-Shank Neural Probe,” *Solid*
327 *State Electronics*. 2017.
- 328 10. R.R. Richardson, J.A. Miller, and W.M. Reichert, “Polyimides as biomaterials: preliminary
329 biocompatibility testing,” *Biomaterials*, **14**(8), 627-635 (1993).
- 330 11. K.C. Cheung, P. Renaud, H. Tanila, and K. Djupsund, “Flexible polyimide microelectrode array for
331 in vivo recordings and current source density analysis,” *Biosensors and Bioelectronics*, **22**(8), 1783-
332 1790 (2007).
- 333 12. G. Rios, E.V. Lubenov, D. Chi, M.L. Roukes, and A.G. Siapas, “Nanofabricated Neural Probes for
334 Dense 3-D Recordings of Brain Activity,” *Nano letters*, **16**(11), 6857-6862 (2016).
- 335 13. F. Lisdat, and D. Schäfer, “The use of electrochemical impedance spectroscopy for biosensing,”
336 *Analytical & Bioanalytical Chemistry*, **391**(5), 1555-1567 (2008).

- 337 14. Z. Xiang et al., "Ultra-thin flexible polyimide neural probe embedded in a dissolvable maltose-coated
338 microneedle," *Journal of Micromechanics and Microengineering*, **24**(6), 065015, (2015)
- 339 15. M.L. Huffman and B.J. Venton, "Carbon-fiber microelectrodes for in vivo applications," *The Analyst*,
340 **134**(1), 18-24 (2009).
- 341 16. N. Burblied, "Coatings of Different Carbon Nanotubes on Platinum Electrodes for Neuronal Devices:
342 Preparation, Cytocompatibility and Interaction with Spiral Ganglion Cells," *Plos ONE*, **11**(7), 1-22
343 (2016).
- 344 17. G. Slaughter, D. Gupta, T. Kulkarni, and L.L. Morton, "A microfabricated low-cost Au nanotip
345 pyramidal electrode array using anisotropic etching for enhanced performance of a glucose
346 biosensor," *Proc. SENSORS, IEEE* **2015**, 1-4 (2015).
- 347 18. G.T.A. Kovacs, "Introduction to the theory, design, and modeling of thin-film microelectrodes for
348 neural interfaces," in *Enabling Technologies for Cultured Neural Networks*, D.A. Stenger, T.
349 McKenna, Eds., Academic Publishers; New York, 121-165 (1994).
- 350 19. B. He, *Neuron Engineering*, Kluwer Academic, Norwell, MA, (2005).
- 351 20. R.L. White and T.J. Gross, "An evaluation of the resistance to electrolysis of metals for use in
352 biostimulation microprobes," *IEEE Transactions on Biomedical Engineering*, **6**, 487-490 (1974).
- 353 21. S.S. Stensaas, and L.J. Stensaas, "Histopathological evaluation of materials implanted in the cerebral
354 cortex," *Acta neuropathologica*, **41**(2), 145-155 (1978).
- 355 22. A.K. Ahuja, M.R. Behrend, J.J. Whalen, M.S. Humayun, and J.D. Weiland, "The dependence of
356 spectral impedance on disc microelectrode radius," *IEEE Transactions on Biomedical Engineering*,
357 **55**(4), 1457-1460 (2008).
- 358 23. A.R. Rahman, J. Register, G. Vuppala, and S. Bhansali, "Cell culture monitoring by impedance
359 mapping using a multielectrode scanning impedance spectroscopy system (CellMap)," *Physiological*
360 *Measurement*, **29**(6), S227-S239 (2008).

361

362

363 **Gymama Slaughter** is currently an Associate Professor of Computer Engineering at the
364 University of Maryland Baltimore and Director of the Bioelectronics Laboratory. Dr.
365 Slaughter's research has been supported by the National Science Foundation for her diabetes
366 research that focuses on the design and development of self-powered glucose biosensor,
367 especially in relationship to monitoring blood glucose in diabetics. She is the recipient of the
368 National Science Foundation's prestigious CAREER AWARD.

369

370 Biographies and photographs for the other authors are not available.

371

372

373 **Caption List**

374

375 **Fig. 1** Schematic design of the flexible neuroelectronic probe structure and CAD layout showing
376 the electrode sites, interconnect traces and bond pads.

377 **Fig. 2** Schematic illustration of the major processing steps in the fabrication of the 64-site probe.

378 **Fig. 3** SEM micrographs of neuroelectronic probe shank with 16 recording electrode sites and
379 submicron interconnect traces sandwiched between two polyimide layers and insert views of
380 shank tip and rectangular pyramid shaped electrode.

381 **Fig. 4** Flexible and optically transparent polyimide neuroelectronic probe accommodates
382 associated bond pads, interconnect traces 10 μm to 1 μm in two distinct metallization layers, and
383 the traces are connected to the electrode sites..

384 **Fig. 5** Flexible and optically transparent polyimide neural probe packaging..

385 **Fig. 6** Recording electrode site before (left) and after (right) MWCNT deposition.

386 **Fig. 7** EIS measurement of six electrodes on a single probe shank before and after MWCNT
387 deposition on a logarithmic scale.

